Science of the Total Environment 908 (2024) 168237

Contents lists available at ScienceDirect

Science of the Total Environment

journal homepage: www.elsevier.com/locate/scitotenv

A combined stability function to quantify flood risks to pedestrians and vehicle occupants

Barry Evans [a,*], Arthur Lam [b], Charles West [c], Reza Ahmadian [b], Slobodan Djordjević [a], Albert Chen [a], Maria Pregnolato [d,e]

[a] University of Exeter, Centre for Water Systems, EX4 4QF, UK
[b] Cardiff University, School of Engineering, Cardiff CF24 3AA, UK
[c] Mott MacDonald, 10 Temple Back, Redcliffe, Bristol BS1 6FL, UK
[d] Delft Univ. of Technology, Dept. of Hydraulic Engineering, Delft 2628 CN, Netherlands
[e] University of Bristol, Dept. of Civil Engineering, Bristol BS8 1TR, UK

HIGHLIGHTS

- Analysis of vehicle and pedestrian stability functions
- Derivation of risk metrics for quantifying and visualising risks posed to vehicle occupants from flooding
- Shows how risks posed to vehicle occupants from flowing flood waters can potentially increase within minutes
- Simulated 1 in 20-year (historical) and 1 in 100-year (synthetic) rainfall event within the city of Exeter (UK)

GRAPHICAL ABSTRACT

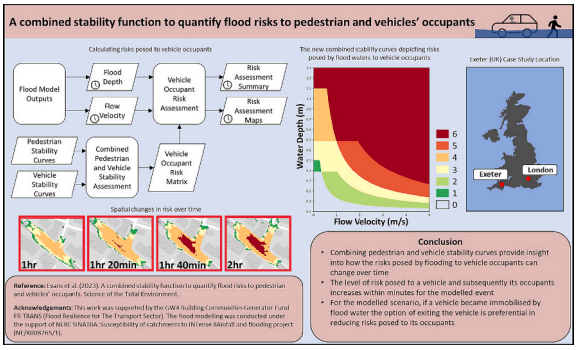

ARTICLE INFO

Editor: Ouyang Wei

Keywords:
Natural hazards
Flood modelling
Transportation
Vehicles
Pedestrians
Stability
Risk

ABSTRACT

With the increase of the frequency and severity of flooding events, coupled with population growth, the risks posed to people from flooding is ever more apparent. This paper proposes a methodology to examine the risks posed to vehicles' occupants and pedestrians simultaneously in an urban context. Through considering stability functions of a range of vehicle types and pedestrian, a risk assessment profile for a vehicle occupant was derived. Using a historical 1-in-20-year rainfall flood event that took place in the city of Exeter (UK) in 2014, and a synthetic 1 in 100-year rainfall flood event, the potential risks posed to vehicle occupants were analysed. The results showed that for these events the potential risks posed to people travelling by car and caught in flood waters were likely to be more severe if they were to remain within their vehicles than if they were to exit said vehicles. Analysis of the changes in risk over time further revealed that if a vehicle was to become immobilised in flood water, they would only have a short timeframe (~10 min) before the level of risk increases. This is a critical finding, highlighting that remaining inside an immobilised vehicle during flood event and waiting for assistance may increase the level the risk the individual is exposed to, with the results showing the significance of such studies in reducing the risk of flooding to people.

* Corresponding author.
E-mail address: b.evans@exeter.ac.uk (B. Evans).

https://doi.org/10.1016/j.scitotenv.2023.168237
Received 29 June 2023; Received in revised form 8 September 2023; Accepted 29 October 2023
Available online 4 November 2023

1. Introduction

The scale, frequency and severity of natural disasters have risen progressively over the last 20 years, and it is likely to increase due to rapid urbanisation and climate change. Floods accounted for 43 % of natural disasters between 1995 and 2015 and affected more population (2.3 billion) than all other natural disasters combined, for a total economic damage of 662 billion USD (Centre for Research on the Epidemiology of Disasters United Nations Office for Disaster Risk Reduction, 2015). Recently, catastrophic floods occurred in China and western Europe in year 2021. For example, in Germany and Belgium in mid-July over 150 mm of rainfall was recorded within 24 h; the excessive rainfall led to flash floods and landslides (Cornwall, 2021) with a total of US$ 6.5–7.7 billion estimated economic loss and 239 casualties (Aon, 2021). Extreme floods in China in June–August in the Henan Province claimed 302 lives and caused extensive damage to properties and critical infrastructure (Aon, 2021).

Urban areas are expected to experience more severe flooding in the coming future, likely because of climate change and urbanisation. The Met Office predicted an increase in extreme rainfall intensity by 20–30 % for England and Wales over the next 20–30 years (HM Government, 2016). Also, the United Nations (UN) reported that the urban population exceeds the rural population globally, and the percentage of urban population would increase from 51 % to 68 % of the global population in 2011–2050 (UN Department of Economic and Social Affairs/Population Division, 2012). The rapidly escalating cost of disasters is an increasing cause for concern for governments, but the true costs of a disaster are felt most acutely at community level and are determined by the community's preparedness and ability to face the event (Arrighi et al., 2021).

The "activity" of individuals is one of the vulnerability factors which are fundamental for analysing the causes of flood fatalities, in addition to age and gender (Jonkman and Kelman, 2005). This activity regards the action that a person may take, e.g. walk away from the floods, stay at home or drive through floodwater. Vehicle-related deaths are a dominant cause of fatalities during flood events, followed by fatalities occurred "in homes, on campsites, when crossing bridges or when walking through floodwaters" (Jonkman and Kelman, 2005: 78). Fitz-Gerald et al. (2010) reported that in Australia (1997–2008) 48.5 % fatalities related to motor vehicles and 26.5 % fatalities were due to inappropriate or high-risk behaviour during floods.

Impacts of flooding on traffic flows and transportation networks can be classified into direct and indirect impacts. Direct impacts can occur when the flood water makes contact with vehicles causing physical damage directly to the vehicle through water damage or indirectly through the vehicle becoming buoyant and colliding with urban elements (Martínez-Gomariz et al., 2017). Indirect impacts could be as a result of increased congestion in the road network through disruption of traffic flows (Pyatkova et al., 2019a, 2019b; Vamvakeridou-Lyroudia et al., 2020), including additional air pollution.

Traditionally, direct impact of flooding on pedestrians, vehicles and infrastructure has been evaluated solely by water depth (e.g. Hammond et al., 2015; Evans et al., 2020), primarily quantified in terms of monetary losses. However, the direct impacts posed to pedestrians and vehicles can be defined with respect to the risk of them being swept away by flood water (i.e., pedestrian or vehicle instabilities), potentially resulting in physical damage and/or loss of life. For pedestrians, two modes of instability have been identified, namely toppling, and sliding (Jonkman and Penning-Rowsell, 2008; Cox et al., 2010; Xia et al., 2014) (Fig. 1). Toppling instability occurs when the moment acted by flood flow on the pedestrian exceeds the resisting moment of the person's effective body weight (i.e. body weight modulated by buoyancy, slope and human positioning); sliding instability occurs when the force of flood flow acting on a person exceeds the frictional force between the pedestrian feet and the ground surface.

The vehicle instability can be classified into three modes, namely floating, sliding and toppling (Shand et al., 2011). Similar to pedestrian's instability, the thresholds of flood water depths and velocities for vehicle instabilities have been developed with empirical and mechanistic approaches (Abt et al., 1989; Keller and Mitsch, 1993; Xia et al., 2014; Shah et al., 2021). When a vehicle is partially submerged in flood water, it is subjected to four forces: (i) buoyancy force; (ii) the force of flood flow; (iii) frictional force resisting the flood force; (iv) the vehicle's weight. The proportion of these four forces governs the mode of instability for the vehicle (Fig. 2). Sliding failure occurs when the flood flow velocity is high and water depth is relatively low; floating failure occurs when the water depth is high enough to lift a vehicle; toppling instability usually occurs when the vehicle is already under sliding or floating (Shand et al., 2011).

In terms of using vehicle and pedestrian stability criteria for emergency management at urban scale, past research utilised hydraulic models and vehicle instability criteria (of specific vehicles) to evaluate risk of vehicles under flooded conditions (Teo et al., 2013; Bocanegra and Francés, 2021). Some other studies developed flood hazard ratings considering both flood water depth and velocity (e.g. Xia et al., 2014; Martínez-Gomariz et al., 2016, 2017, Stevens et al., 2020; Musolino et al., 2020; Wang et al., 2021), especially for evacuation planning. Previous work (Pyatkova et al., 2019a, 2019b; Pregnolato et al., 2017) reviewed literature relating to maximum vehicle speed and flood depth; it highlighted that when water depths are above a threshold value, then there is an increased likelihood that vehicles will stall/breakdown and become trapped within flood water. This threshold value is dependent on the make and model of vehicle, which can be as low as 15 cm of flood depths for smaller vehicles and up to 40 cm for SUVs for example. Once a vehicle becomes immobilised due to flood water, the occupant/s will either choose to remain within or exit the vehicle. Due to the dynamic nature of flooding events, the time required to act and minimise risks posed to the occupant/s can vary. Wang et al. (2021) compared the pedestrian and vehicle hazard ratings and applied the two rating to two

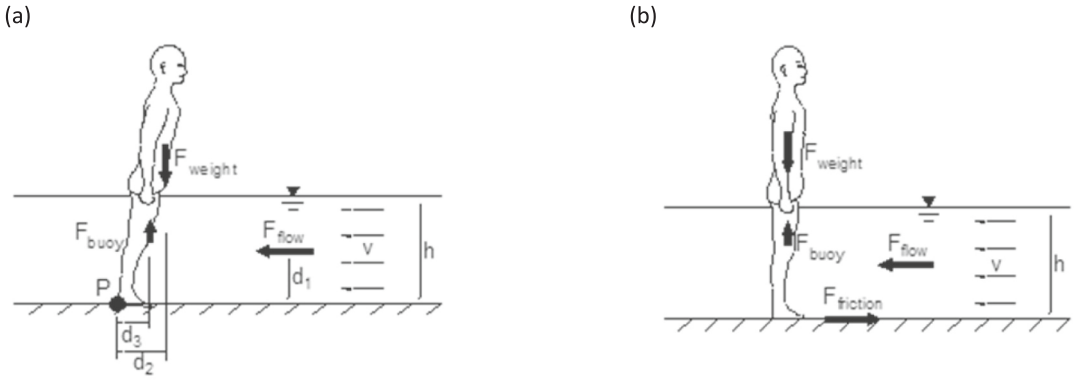

Fig. 1. The modes of pedestrian instability: (a) toppling; (b) sliding (Jonkman and Penning-Rowsell, 2008; Xia et al., 2014).

flooding cases, but they did not establish a joint pedestrian-vehicle hazard rating. Lazzarin et al. (2022) proposed an impact parameter to quantify flood hazard accounting for both water depth and velocity; they derived the relative damage as a function on this parameter for different exposed elements (people, vehicles, and buildings). These functions provided limit stability conditions, but without discretisation (stable/unstable only); in addition, the method was not demonstrated for an urban area or case study. In conclusion, the joint hazard ratings of pedestrians and vehicles have not been deeply studied, in particular in relation to the dynamic nature of flooding risk.

This study presents an improved methodology to depict risks posed by floodwater to vehicle occupants via the use of combined water depth and velocity stability curves, considering the direct impact of flooding to people as a joint risk to pedestrians and vehicles. This paper establishes a joint pedestrian-vehicle hazard rating and applies the rating to a real flooding case. The method originally considers both flood depth and flow velocity of floodwaters and how they dynamically change during a flood event. The resulting assessment, derived from the stability curves, provides a preliminary guide for evaluating risks to vehicle occupants and how this changes dynamically.

This paper aims to understand the combined risk of flood depth and velocity to vehicle occupants considering the stability functions of both vehicles and pedestrians simultaneously. In this approach, the risk assessment considers the vehicle being swept away either before the occupant has exited the vehicle or still within close proximity to the vehicle, or the occupant is swept away upon exiting the vehicle.

The main objectives of the study include: (i) to assess and compare the hazard to vehicles and pedestrians considering flood depths and velocity; (ii) to quantify the risks posed to vehicle occupants using both vehicle and pedestrian stability analysis; (iii) to provide insights about how to use this research in practice. The study is conducted with the combination of a flood model and vehicle/pedestrian stability criteria. The vehicle hazard ratings are compared to the pedestrian hazard ratings to provide an initial guidance on whether a driver should abandon their vehicle if the vehicle hazard rating is higher than the pedestrian one. The method was applied to Exeter, a city in the south-west of the UK which is city susceptible to flooding, with the results demonstrating an exemplar application.

2. Methodology

This section outlines the approaches used for combining pedestrian and vehicle stability curves to derive the potential risks posed to vehicle occupants from flooding. This section is divided into three sub-sections (Fig. 3). Section 2.1 describes the flood model and flood scenario that were employed for the analysis presented in this paper. Section 2.2 explains how the pedestrian and vehicle stability curves are combined to evaluate the risks to vehicle occupants. Section 2.3, defines the assessment illustrating how the integration of the flood model outputs and derived risk matrix provides valuable insights into the potential risks posed by flooding to vehicle occupants; finally, we suggest appropriate courses of action to mitigate these risks.

2.1. Flood modelling

The flood modelling within this paper was carried out using the Urban Inundation Model (UIM) outlined in Chen et al. (2007), that uses a simplified approach to solve the 2D diffusion wave equation, that has been benchmarked against other models that provide "full" mathematical representation of the physical processes controlling floodplain inundation such as TUFLOW, MIKE FLOOD, and SOBEK, and provides water level and flow velocity values similar to predictions made by these models Néelz and Pender (2010). The two flood scenarios used in this case study consist of one derived from data of a historical event that occurred in Exeter (UK) on the 16th October 2014 as detailed in Chen et al. (2016) and a synthetic 1 in 100-year design storm event over the same catchment area. During the historical event, the peak rainfall intensity over a 30-minute duration was equivalent to an estimated design rainfall of a 1 in 20-year event. Fig. 4a and b shows the average rainfall hyetographs applied across the catchment area for the two modelled scenarios. The hyetograph for the historical 1 in 20-year event was derived from 28 spatially distributed radar cells (Met Office, 2003), calibrated by the observation at a local rain gauge (Melville-Shreeve, 2014).

The flood model extent was centred over the Heavitree area of Exeter in the UIM simulation, using the Environment Agency's LiDAR data (Environment Agency, 2013) and Ordnance Survey Topography data (Ordnance Survey, 2014) for model building. The model extent consists of 29,793,710 grid cells at a $1m^2$ resolution. The case study is an independent catchment with no back water effect observed during the event, such that the downstream boundary condition was set as free outfall. Fig. 5a shows the location of Exeter and displays the flood extent resulting from a 4-hour simulated 1 in 20-year event, highlighting the maximum recorded depths within the simulated area. Additionally, a zoomed-in section of the city (Fig. 5b) is included to demonstrate the magnitude of localised flooding for this event along specific sections of the road network.

The outputs of the flood models were set to 1-minute intervals outputting flood-depth values for each cell and the corresponding flow velocities across the East and North cell boundaries over a simulated event period of 4 h. To calculate the stability values both the flood depths and surface flow velocities are required. The UIM uses a finite difference approach and produces three separate raster-grid file types for each specified time-interval as outputs. These three files consist of water-depths and flow velocities in the x (U) and y (V) directions at the East and North cell boundaries respectively. To determine the flow velocity magnitude (U_m) within a grid cell, the flow velocities in the x direction (U) and y direction (V) across the cell boundaries are considered with U_m calculated as shown in Eq. (1):

$$U_m = \sqrt{\left(\frac{U_{x-1,y} + U_{x,y}}{2}\right)^2 + \left(\frac{V_{x,y-1} + V_{x,y}}{2}\right)^2} \quad (1)$$

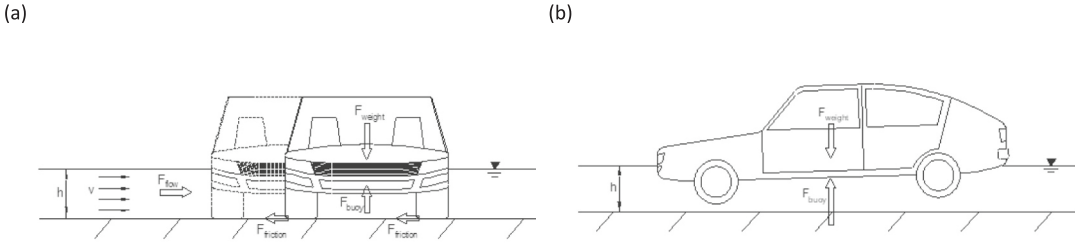

Fig. 2. The modes of vehicle instability: (a) sliding; (b) floating (Shand et al., 2011).

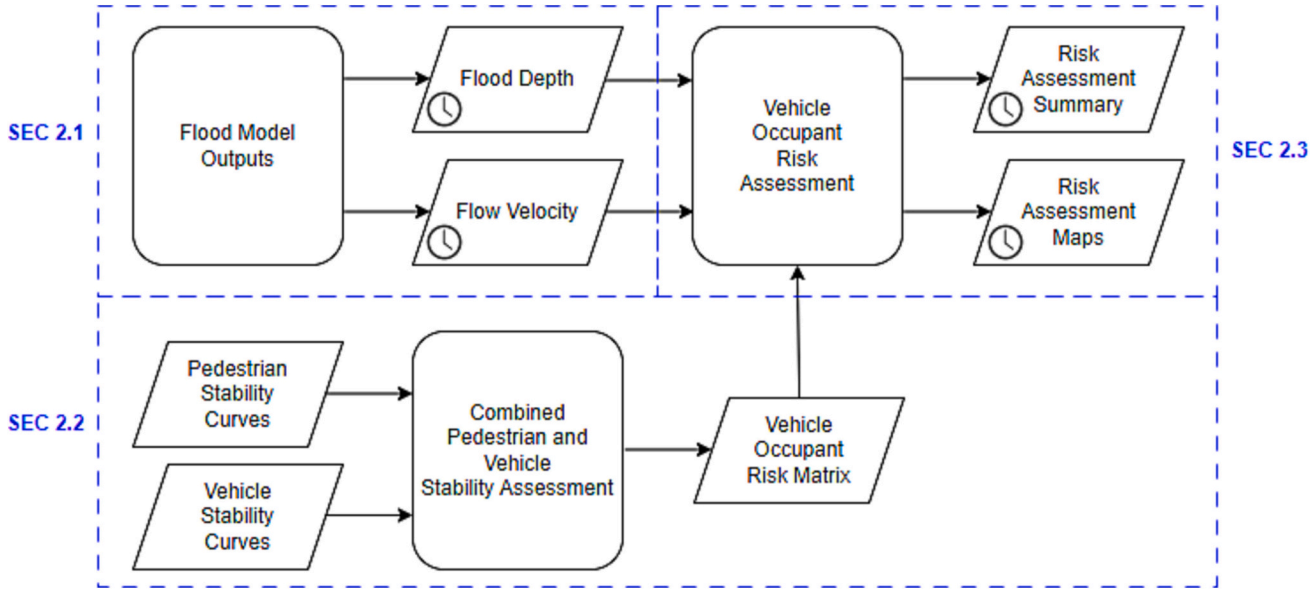

Fig. 3. Procedure adopted by this paper to quantify risks posed to individuals travelling by car and on foot.

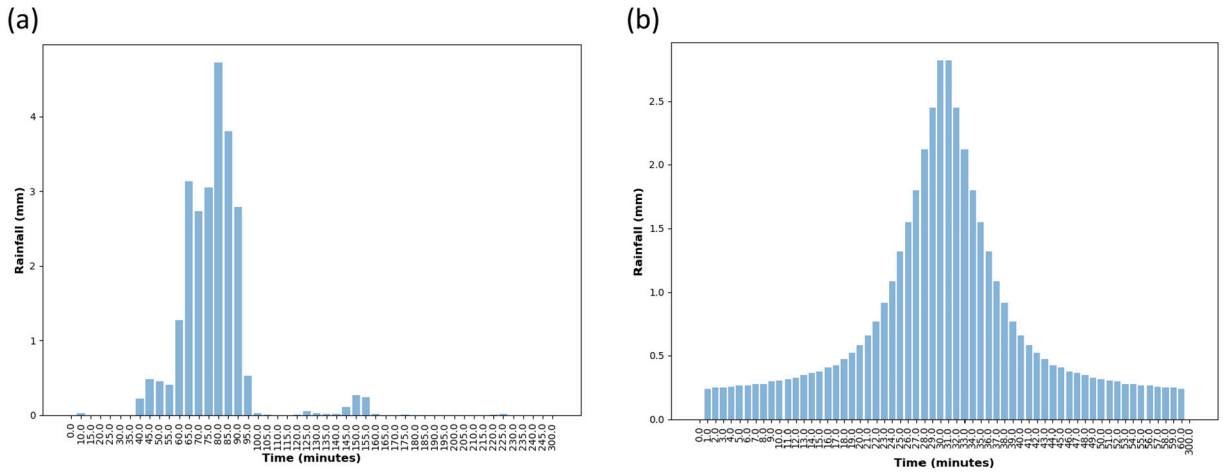

Fig. 4. Average rainfall hyetographs over catchment for the (a) 1 in 20-year historical event and (b) 1 in 100-year synthetic design rainfall event.

2.2. Risk classification

The risks posed to both the vehicle and its occupant/s from flood water is not solely limited to flood depth but also dependent on the flow velocity of the floodwater. It is shown that such risks are generally underestimated when only depth is used to assess the risk in fast-flowing flash floods (Musolino et al., 2020). The combined effect of flood depth and flow velocity of encompassing floodwater can result in either the individual or the vehicle being swept away either, as a result of the force applied by moving water overcoming the frictional coefficients between the car tyres of a vehicle, or feet of an individual, and the road surface, or the depths of the flood water being sufficiently high that either the car or individual becomes buoyant, or a combination of the two. While there are two types of stability models as mentioned in Section 1, the empirical stability models by Martínez-Gomariz et al. (2016) and Martínez-Gomariz et al. (2017) were selected in this research. It is because the flood simulated is a high-water-depth (reaching up to 3 m), low-flow-velocity (<1 m/s) flood, and empirical stability models were shown to give more conservative hazard ratings in such flood cases (Lam et al., 2022). The vehicle hazard rating (Martínez-Gomariz et al., 2017) is:

$$FHR_v = vy = 0.0158 \times SC_v + 0.32 \tag{2}$$

where FHR_v is vehicle flood hazard rating; v is flow velocity (m/s); y is water depth (m); SC_v is a stability coefficient which considers the properties of the vehicle (kg/m). SC_v is defined as:

$$SC_v = \frac{GC \times M_c}{PA} \times \mu \tag{3}$$

where GC is the ground clearance (m); M_c is the kerb weight (kg•m/s^2); PA is the vehicle plan area (m^2); μ is the dimensionless friction coefficient between the tyre and ground. Besides Eqs. (2)–(3), vehicles are known to be unstable with no velocity if the water depth is beyond the buoyancy depth h_b (m) which is defined as:

$$h_b = \frac{M_c}{\rho_w \times l_c \times b_c} + GC \tag{4}$$

where ρ_w (kg/m^3) is water density, l_c (m) is vehicle length, and b_c (m) is the vehicle width. In this research, Eqs. (2)–(5) are assumed to fully specify the stability of vehicles.

Regarding pedestrians, the considered hazard rating (Martínez-

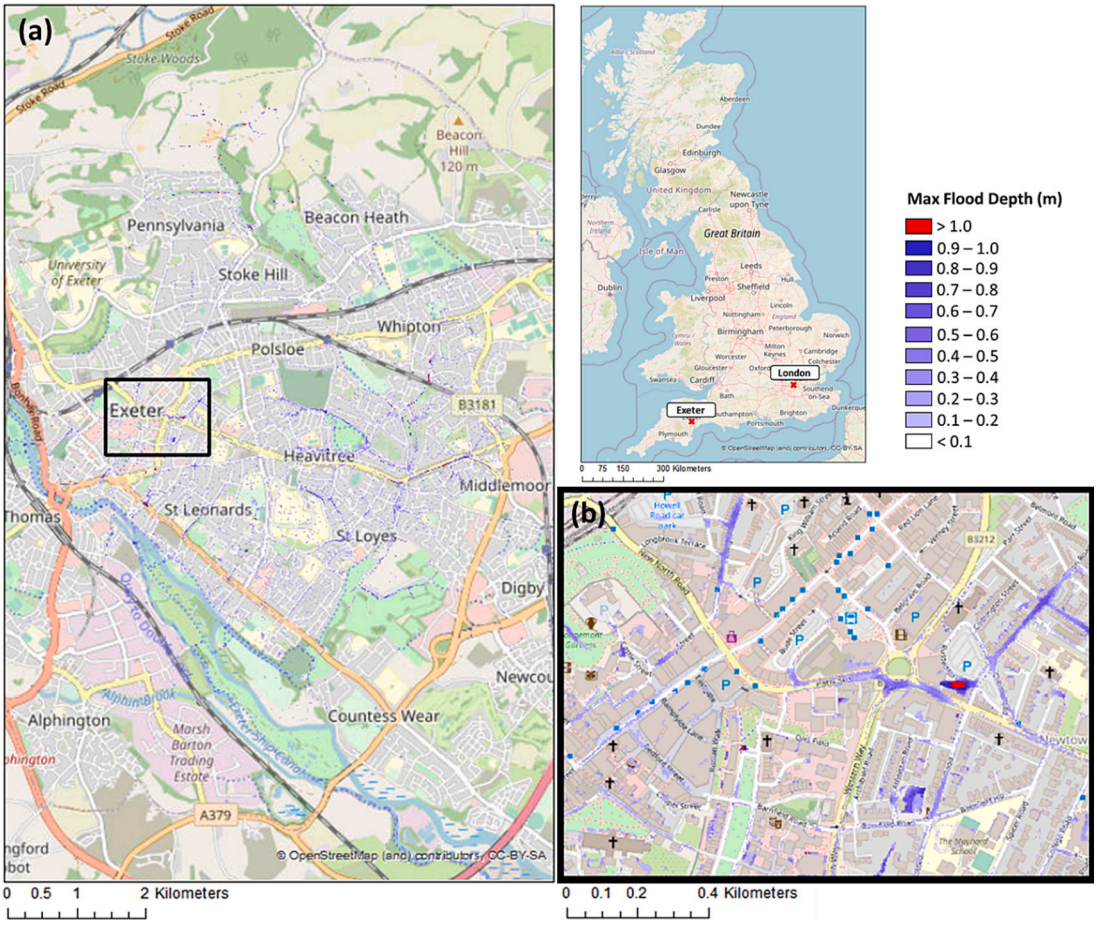

Fig. 5. Location of Exeter, modelled extent (a) and zoomed in region highlighting a flooded road area (b); derived from 1 in 20-year historical event.

Gomariz et al., 2016) is:

$$FHR_p = vy = \left(0.0027 \times SC_p + 0.31\right)^2 \quad (5)$$

where FHR_p is the pedestrian hazard rating; SC_p is the pedestrian stability coefficient, defined as:

$$SC_p = P \times H \quad (6)$$

where P and H refer to the weight (kg) and height (m) of the pedestrian with the values for P ranging from 16.2 kg to 100 kg and H from 1.09 m to 1.90 m in this paper. Similar to vehicles, pedestrians are considered to be "unstable" in standing water, if the water depth is beyond the theoretical buoyancy depth. The lower and upper limits of theoretical buoyancy depth are set to be 0.5 m and 1.2 m for pedestrians (Cox et al., 2010).

With the large variety of vehicles in terms of make/model, and their corresponding physical characteristics, there is no singular stability curve that can be used to define their physical behaviour/response to flood waters, the same is also true for that of people as well with individuals varying both in height and body mass. To capture these variances, Martínez-Gomariz et al. (2017) identified three zones using stability curves:

1. Safety Zone: vehicle/pedestrian is at low risk of becoming unstable.
2. Uncertainty Zone: vehicle/pedestrian is at potential risk of becoming unstable.
3. Instability Zone: vehicle/pedestrian is at high risk of becoming unstable.

Fig. 5 shows the stability curves and zones for vehicles and pedestrians respectively, which were derived considering a variety of vehicle types and pedestrian height and weight variations.

To quantify the risks posed to vehicle occupants in this study, we consider both vehicle and pedestrian stability curves simultaneously. Here we examine a "what if" scenario whereby if a vehicle was immobilised during a flood event and in contact with floodwater, how would the risks posed to the vehicle occupant change over time based on whether they remain in or exit the vehicle. Based on risk classes for both vehicles and pedestrians, seven risk score values ranging from zero to six are defined, as shown by Table 1. In this table, a risk score of zero relates to where the combination of depths and velocity are so low that they pose little to no risk to both pedestrians and stationary vehicles based on their respective stability curves. The generated risk scores are based on the combination of hazard classes for both vehicles and pedestrians.

2.3. Dynamic changes to risks

The selected flood modelling software used within this study (UIM) outputs both the flood depths and flows velocities at regular user-defined intervals, within a combination of raster files (Chen et al., 2007). Through post-processing of the flood model's velocity and depth outputs each grid cell is assigned a risk score for each time interval. The flood model produces at 1-minute time intervals resulting in 240 risk-based raster files for the 4-hour flood event.

With variations in both flood depths and flow velocities over the course of the flood event, the level of risk posed to individuals will change over time. Considering a scenario where a vehicle has stopped/become immobilised within flood water, the occupant would need to assess the risks posed to themselves, how these risks may change over time, and take appropriate course of action. Within this paper, the time

Table 1
Quantifying risks posed to vehicle occupants.

Risk Score	Vehicle Risk Class	Pedestrian Risk Class	Derived Risk Class
0	Safety Zone	Safety Zone	Low risk of vehicle instability Low risk to occupant exiting vehicle
1	Uncertainty Zone	Safety Zone	Medium risk of vehicle instability Low risk to occupant exiting vehicle
2	Safety Zone	Uncertainty Zone	Low risk of vehicle instability Medium risk to occupant exiting vehicle
3	Uncertainty Zone	Uncertainty Zone	Medium risk of vehicle instability Medium risk to occupant exiting vehicle
4	Instability Zone	Uncertainty Zone	High risk of vehicle instability Medium risk to occupant exiting vehicle
5	Uncertainty Zone	Instability Zone	Medium risk of vehicle instability High risk to occupant exiting vehicle
6	Instability Zone	Instability Zone	High risk of vehicle instability High risk to occupant exiting vehicle

from the moment a vehicle becomes stuck, and the time taken for the occupant to act before the level of risk increases is regarded as the "reaction time". Ignoring additional external risks, such as that posed by other road users, the occupant of the vehicle will decide whether to remain within the vehicle or to exit the vehicle.

Within the scope of this study the minimum reaction time is defined as the time taken from the first instances the risk value within a grid cell is greater than zero to the time taken for the risk value within that cell to increase, with subsequent additional "reaction times" following between further risk increase transitions.

3. Results

The combination of the vehicle and pedestrian stability curves (Fig. 6a, b) and the classification of Table 1 are integrated to produce the risk curves outlined in Fig. 7. These risk curves comprise of both depth and flow velocity components, presenting a more comprehensive depiction of risks to both pedestrians and vehicles in contrast to just considering flood depths (as considered in precedent literature). They depict in fact risks posed by floodwaters to vehicle occupants, considering them as drivers and potential pedestrians. The combination of stability curves/risk classification reveals that the area corresponding with a risk score of one is comparatively small and implies that relatively small increases in the flow velocity or depth can result in an increased risk (to a risk score of three) with both the vehicle and its occupant now being within the uncertainty zone.

3.1. Application to the case study

The combined stability curves shown in Fig. 7 are applied to the case study in Exeter (see Section 2.1). For assessing the risks posed to vehicle occupants the analysis is focused solely on grid cells that lie within the transportation network (along road surfaces). In considering risk as a dynamic entity, Fig. 8a highlights the changes, depicting the counts of the grid cells along road surfaces for the 1 in 20-year event, with risk scores greater than zero over time, where we observe the initial increase in the count of risk score 1 with increases in scores 3, 4, and 6 following. Additionally for this flood event we notice only a slight increase in a risk score of 2 and an absence of risk score 5. Fig. 8b shows the risk score classifications for the 1 in 100-year synthetic event that shows a comparative distribution of risk scores though at increased magnitudes.

During the modelled flood event, the risk scores associated to each grid-cell can vary. A vehicle immobilised within floodwater within grid cells that have a corresponding risk score of 1 at time t may only have a short amount of time (Δt) before either the depth and/or velocity of the flood water changes enough to increase the level of risk that the vehicle and its occupant are exposed to. This Δt equates to the reaction time whereby the vehicle occupant will take a course of action, such as to exit

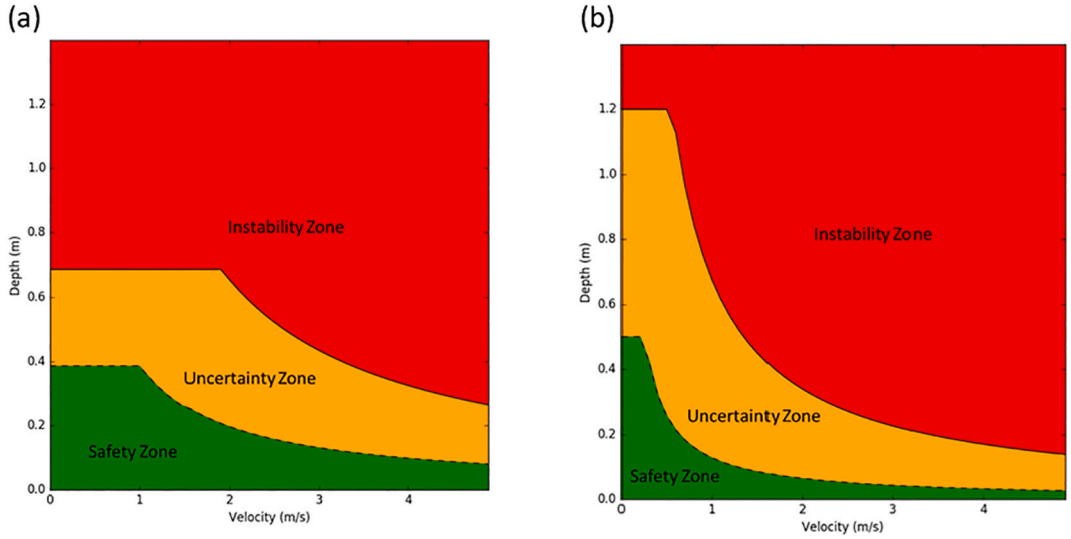

Fig. 6. Applied stability curves for (a) vehicles (from Martínez-Gomariz et al., 2017); and (b) pedestrians (from Martínez-Gomariz et al., 2016).

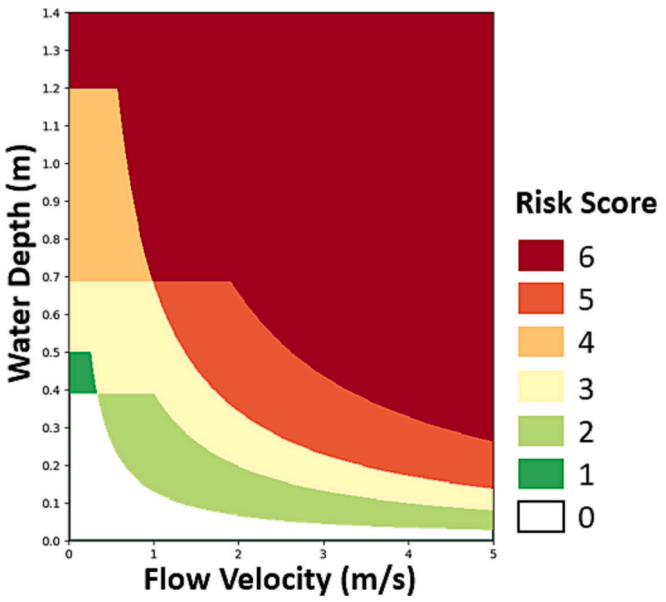

Fig. 7. The new combined stability curves depicting risks posed by flood waters to vehicle occupants.

or remain within the vehicle before the level of risk increases. Fig. 9 shows a comparison of how the risks change within a section of the road network over the first 2 h for the 1 in 20-year event (a) Vs the 1 in 100-year event (b). At this highlighted location, along Holloway Street, we observe localised flood depths of >40 cm and initial risks developing between 1 h 20 min and 1 h and 40 min in the 1 in 20-year event with majority of risk score values of 1 and 3 showing uncertain risks posed to both pedestrians and vehicles. Within the next 20 min the region has transitioned to a risk score of 4 now placing vehicles within the "instability zone", meaning that for all vehicle types considered in this study there is increased likelihood that the vehicle could either become buoyant and/or begin sliding along road surface in an uncontrolled manner. For the 1 in 100-year event, within the first hour of the event, the region is already showing risk scores of 4, where 20 min later we observe transition to risk scores of 6 meaning high instability risks are now posed to both pedestrians and vehicles.

4. Discussion

4.1. Risk curve analysis

Analysing the curves depicted in Fig. 7 and the respective minimum depth and velocity magnitudes for each risk score (Table 2) highlights that only risk scores 2 and 5 have a minimum velocity > 0. These risk scores both correspond to higher risks posed to pedestrians than vehicles highlighting that pedestrians are more vulnerable to flow velocities than vehicles as verified in studies outlined in the studies in Martínez-

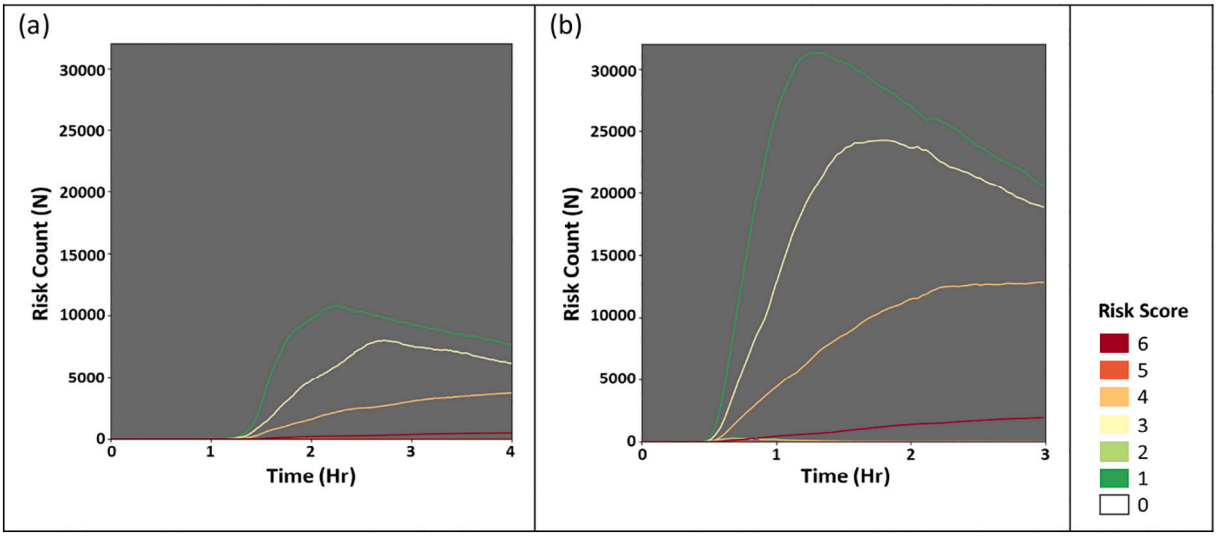

Fig. 8. Risk changes over time for 1 in 20-year event (a) and synthetic 1 in 100-year event (b).

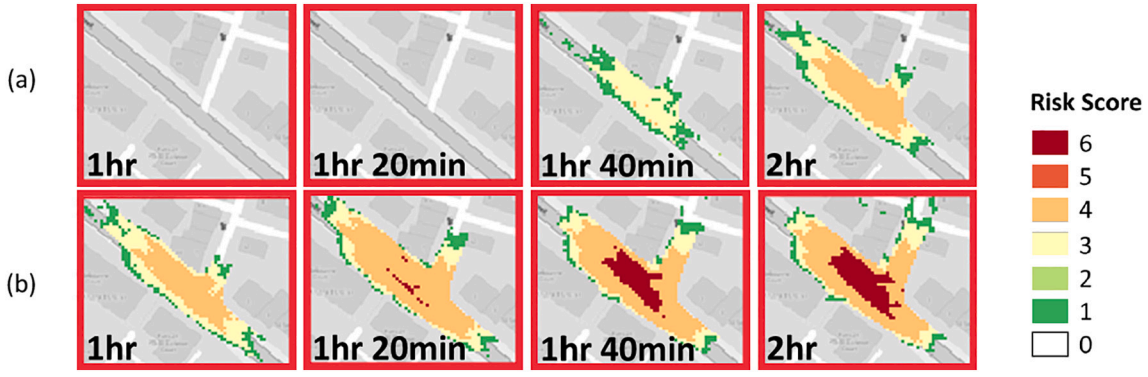

Fig. 9. Visualisation of risk transitions between 1 h and 2 h into flood event for (a) 1 in 20-year event and (b) 1 in 100-year event.

Table 2
Minimum depth and velocity parameters for risk classifications.

Risk score	Min depth (m)	Min velocity (m/s)
0	0.0	0.0
1	0.39	0.0
2	0.03	0.34
3	0.08	0.0
4	0.69	0.0
5	0.14	1.0
6	0.26	0.0

Gomariz et al. (2016) and Martínez-Gomariz et al. (2017).

Table 3 shows the analysis of the risk distribution percentage for the duration of each modelled event where the risks are analysed to determine instances when the risk is higher to pedestrians than vehicles (risk score = 2 or 5), higher to vehicles than pedestrians (risk score = 1 or 4), or equal (risk score = 3 or 6). The distributions show that for the duration of the modelled events, instances where the risk posed to pedestrians are potentially higher than vehicles are the least, around 0.1 %. In contrast the potential risks posed to vehicles are in the majority for both modelled events.

4.2. Consideration of velocity within risk assessments

With the dominant driver of risks during the event being attributed to flood-depths, what is the importance of considering flow velocities when defining risks? To assess this question a comparison is made of deriving risk classifications both with and without velocity considerations. Fig. 10 shows a frequency distribution of the maximum recorded flow velocities for each grid cell during the two modelled events. For the 1 in 20-year event 95.18 % of the recorded maximum velocities are below the 0.34 m/s threshold that is the minimum velocity required to put pedestrians into uncertain instability regions at low flood depths, with 88.65 % of recorded maximum recorded flow velocities being below this threshold velocity for the modelled 1 in 100-year event.

In Fig. 10 we observed most of the recorded maximum flow velocities within cells are within the lower regions with the median value being 0.12 m/s. This is expected to be the main reason that the water depth is the main driver of the flood risk to the vehicle passengers. However, although the velocities of flood water along road surfaces for this event are relatively low, there are instances where its magnitude is such that can push the risk posed to vehicle occupants to a higher risk value, when coupled with flow depth. Fig. 11 shows incidents (represented by points) for both modelled events where the recorded flow velocity within a grid cell during the model run is such that the derived risk score is higher when flow velocities are considered. In this figure we observe that the inclusion of the velocity components within the risk assessments increases the localised risk scores from 0 to 2 and from 1 to 3 respectively, highlighting the significance of incorporating both the floodwater depth and velocity in evaluating the stability of vehicles and pedestrians and identifying the increased risks posed to them. Table 4 shows a summation of the derived risk values over the course of the modelled event when the velocity of the flood water is and is not considered. The table highlights that when velocity is considered we now observe risk classifications with a score of 2 that imply potential instability for pedestrians, and an increase in the number of cells with risk scores of 3.

The modelled flood event in this study is characterised by relatively low flow velocities, wherein changes in flood depths predominantly drive the transition between risk scores. This feature means that most of the flooded areas were classed with a risk score of 1 near the start of the flood. As the localised flood depths increased within these areas, the risk scores transition to 3. Further increases in flood depth causes these areas to attain even higher risk scores, of 4 and then 6. Therefore, flood depth drove the risk score to increase from 1, to 3, to 4 and to 6. This localised risk transition pattern suggests that the risks posed to a vehicle increase at a higher rate than those posed to a pedestrian with pedestrians being more influenced by increases in flow velocity. Thus, remaining in a vehicle stranded in flood water increases the risks to the occupant, due to that it is more likely that the vehicle will become unstable over time than a pedestrian in the same location.

4.3. Dynamic changes in risks

Fig. 9 highlighted that the localised risks that both vehicles and pedestrians are exposed to within a region can increase during the flood event. Previous works have highlighted that when flood depths are >30 cm, there is an increased likelihood that a vehicle in that flood water would breakdown and become trapped in the water. Analysis of the combined stability curve shows that for depths within the range of 30-40 cm, both vehicles and pedestrians are considered to be within the "safety zone" with respect to their stability functions. Therefore, to compare the risks posed to both pedestrians who remain within a vehicle and exit a vehicle once a vehicle has been deemed to become "stuck" in flood water we analysed the time duration for each cell from time of when flood depth within a cell equals 30 cm (but the risk score of zero) to the times when the risk scores within that cell becomes greater than one, potentially putting either the vehicle and/or the pedestrian at increased risk of instability. Figs. 12 and 13 show box plot representations (along with the counts of number of datapoints) of the time elapsed where the corresponding risks posed to occupants of vehicle change, based on whether they stay within or exit the vehicle, with the details of these plots summarised in Table 5. The analysis of this data shows that if a vehicle has been immobilised within water at a depth of 30 cm, there is a greater likelihood that the change in risk level in that region would be more problematic for a vehicle than that of a pedestrian in the same location and that the duration between increased changes in risk scores is shorter for vehicles than it is for pedestrians.

Based on these analyses, if a vehicle were to become immobilised in flood waters, the data suggests that the time elapsed before the vehicle could become unstable is approximately 10 min where in contrast the time when the risks posed to a pedestrian would not increase until about 20 min. This implies that if the vehicle was trapped within flood water, the occupant should exit the vehicle (if safe to do so based on surrounding conditions) and move to a safe location. It should be noted however that this conclusion is derived based on data within this study and the authors do not recommend this as a general rule. Further research is required before it can be applied to other locations.

5. Conclusions

With the risks posed by flooding affecting vehicles and pedestrians differently, we need to consider the method of evacuation during a flooding event. Wang et al. (2021) showed that the severity of the flood risk is the highest for cars, followed by SUVs, children, and adults. This rule agrees with the generalised findings of the analyses within this study where the risks to vehicles and its occupants based on their stability functions were analysed.

The outcome of this research provides additional tools for flood

Table 3
Risk distribution during modelled flood events.

Flood event	Higher risk to pedestrians	Higher risk to vehicles	Equal risk to vehicles and pedestrians
1 in 20-years	0.1 %	64.1 %	35.9 %
1 in 100-years	0.1 %	62.7 %	37.2 %

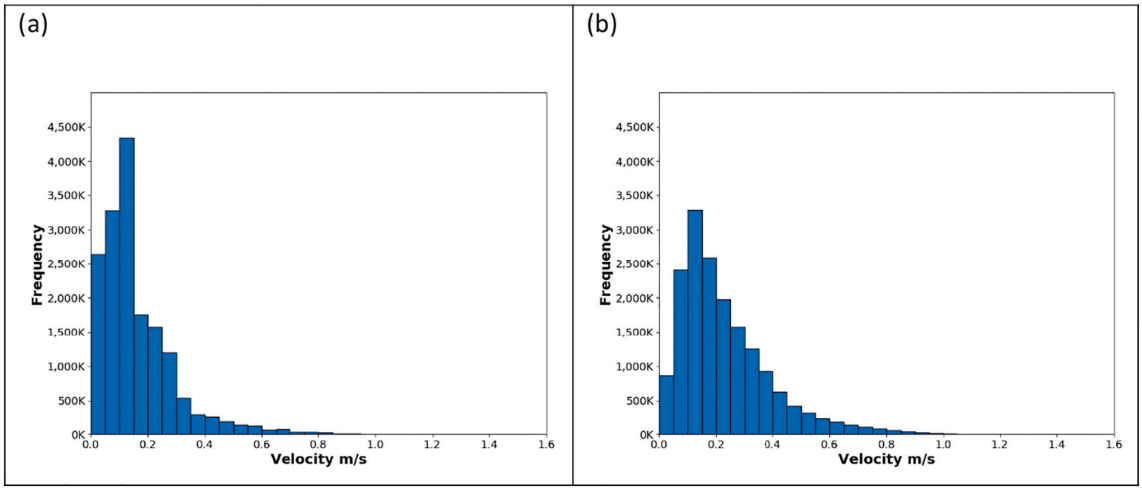

Fig. 10. Max flow velocity distribution for (a) 1 in 20-year flood event and (b) 1 in 100-year flood event.

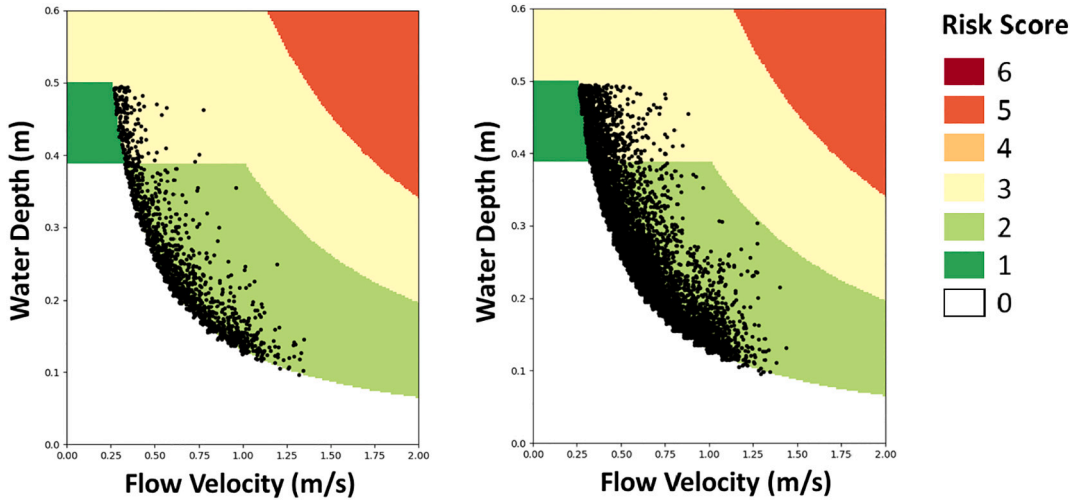

Fig. 11. Instances where the derived risks scores are higher when velocity is considered for (a) 1 in 20-year event and (b) 1 in 100-year event.

Table 4
Comparison of the sum of risk distributions (with and without velocity of floodwater considered) over the course of the modelled event.

Risk score			1	2	3	4	5	6
Cell count	1 in 20 years	Without velocity	1,349,469	0	924,408	384,087	0	46,184
		With velocity	1,349,209	1467	924,668	384,087	0	46,184
	1 in 100 years	Without velocity	1,795,885	0	1,370,341	654,294	0	79,213
		With velocity	1,794,708	5274	1,371,518	654,293	0	79,214

impact assessment to transport networks, while verifying specific modelling hypothesis (e.g. static vehicles, maximum depth of water). We expect this work to be useful to urban planners and authorities that are responsible for emergency management. This paper highlights the development of combined depth-velocity stability curves of pedestrians and vehicles and analysed the risks posed by flooding to vehicle occupants over time within a UK study area. With the stability curves being comprised of both depth and flow velocity components, they present a more comprehensive depiction of risks to both pedestrians and vehicles in contrast to just considering flood depths (as considered in precedent literature). The application of this approach to the case study revealed that even with the relatively low surface flow velocities the flow velocity was high enough to increase the risk exposure in several instances. Therefore, when considering the risk exposure of flooding to vehicle occupants, it is important to consider both the depth and flow velocity of the flood water.

Through analysing the dynamic changes in flood risks during the simulated event, the data showed that, if a vehicle becomes immobilised in flood water, the occupants will have a short timeframe (~10 min) to exit the vehicle before the level of risk they are exposed to increases. This analysis implies that vacating their vehicles and moving away from the risk area on foot is likely to reduce risk exposure more than remaining in the vehicle and waiting for assistance.

The selected flood events for this proof-of-concept study were

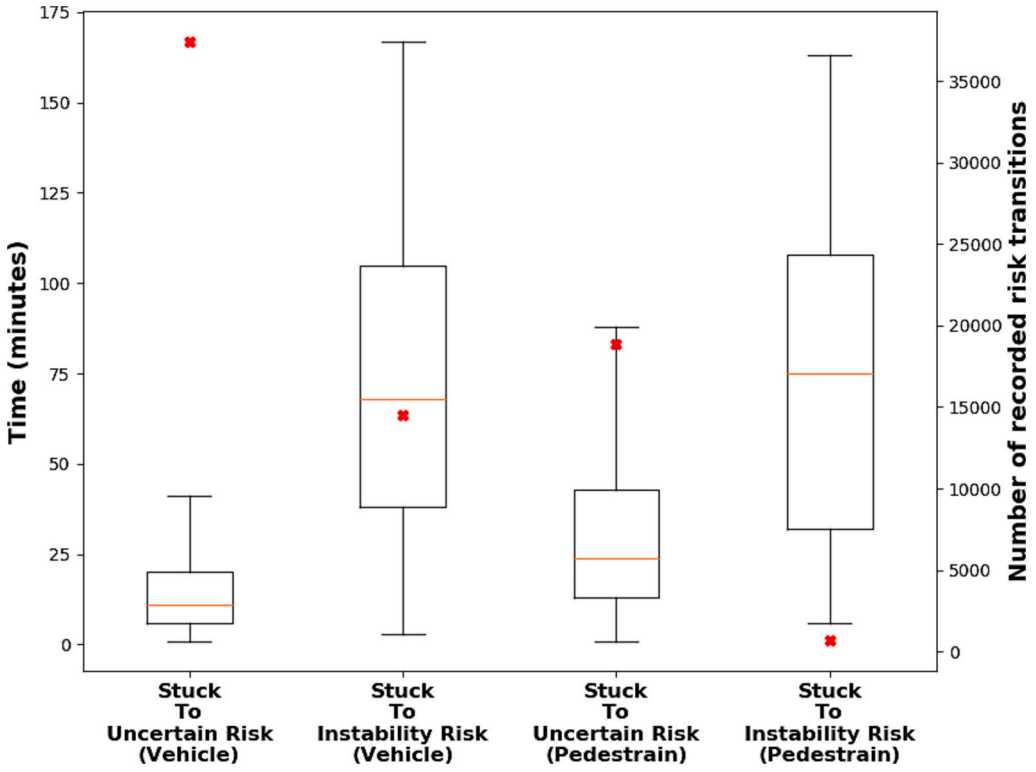

Fig. 12. Risk transitions for 1 in 20-year event.

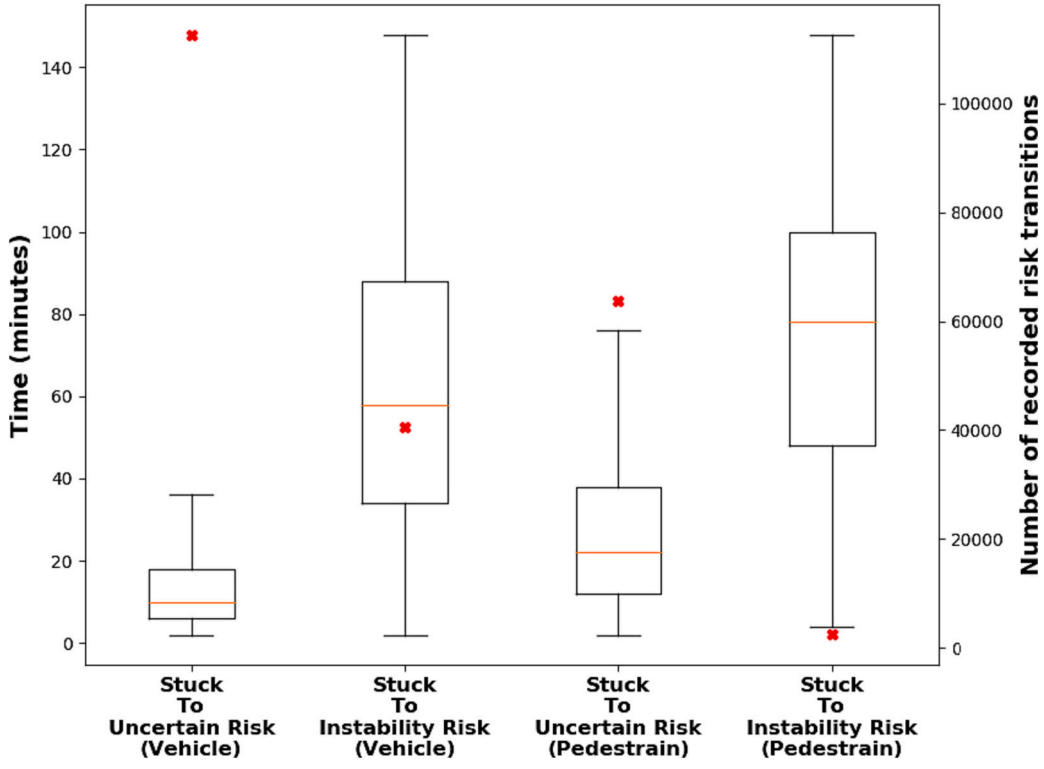

Fig. 13. Risk transitions for 1 in 100-year event.

derived from a 1 in 20-year historical rainfall event and a 1 in 100-year synthetic rainfall event due to the availability of pre-existing data at the time of writing. The approaches outlined in this paper for quantifying risks and analysing risk transitions are transferrable and can be utilised to examine and quantify the risks posed to vehicle occupants in other locations and other flood events on the proviso that both depth and flow velocity values are available for the time interval of interest.

Future work will involve checking and improving this methodology

Table 5
Summary of risk transition times for trapped vehicles within flood water.

		1 in 20-years		1 in 100-yeare	
		Mean transition time (min)	Count	Mean transition time (min)	Count
Vehicle	Stuck to uncertain risk	11	37,453	10	112,654
	Stuck to instability risk	68	14,536	58	40,441
Pedestrian	Stuck to uncertain risk	24	18,870	22	63,635
	Stuck to instability risk	75	651	78	2414

on other real events, including those that contain records of casualties and injuries and damage to vehicles.

CRediT authorship contribution statement

Barry Evans: Conceptualization, Methodology, Software, Investigation, Formal analysis, Writing - Original draft, Visualization.
Arthur Lam: Methodology, Validation, Investigation, Writing - Review & editing,
Charles West: Data Curation, Methodology, Investigation, Writing - Review & editing
Reza Ahmadian: Supervision, Writing - Review & editing
Slobodan Djordjevic: Supervision, Writing - Review & editing
Albert Chen: Supervision, Flood modelling, Software, Writing - Review & editing
Maria Pregnolato: Project administration, Funding acquisition, Supervision, Writing - Review & editing.

Declaration of competing interest

The authors declare that they have no known competing financial interests or personal relationships that could have appeared to influence the work reported in this paper.

Data availability statement

The NIMROD radar rainfall, LiDAR, and Topography data used in the study were under the licenses by British Atmospheric Data Centre, Environment Agency, and the Ordnance Survey, respectively. All other data which are not subjected to non-disclosure agreements with stakeholders, or third parties are available upon request; data sources are clearly specified throughout the paper.

Acknowledgements

This work was supported by the GW4 Building Communities Generator Fund FR-TRANS (Flood Resilience for The Transport Sector) and the ARSINOE (climAte ReSIlient-regioNs thrOugh systEmic solutions and innovations) project, funded by EU H2020 programme (GA 101037424). The flood modelling was conducted under the support of NERC SINATRA: Susceptibility of catchments to INTense RAinfall and flooding project (NE/K008765/1).

References

Abt, S.R., Wittier, R.J., Taylor, A., Love, D.J., 1989. Human stability in a high flood Hazard zone. J. Am. Water Resour. Assoc. 25, 881–890. https://doi.org/10.1111/j.1752-1688.1989.tb05404.x.
Aon, 2021. Global catastrophe recap: July 2021. http://thoughtleadership.aon.com/Documents/20211008_analytics-if-july-global-recap.pdf. (Accessed 6 January 2022).
Arrighi, C., Pregnolato, M., Castelli, F., 2021. Indirect flood impacts and cascade risk across interdependent linear infrastructures. Nat. Hazards Earth Syst. Sci. 21, 1955–1969. https://doi.org/10.5194/nhess-21-1955-2021 (2021).
Bocanegra, R.A., Francés, F., 2021. Assessing the risk of vehicle instability due to flooding. J. Flood Risk Manag. 14, e12738 https://doi.org/10.1111/jfr3.12738.
Centre for Research on the Epidemiology of Disasters United Nations Office for Disaster Risk Reduction, 2015. The Human Cost of Weather-related Disasters 1995–2015.
Chen, A.S., Djordjevic, S., Leandro, J., Savic, D.A., 2007. The urban inundation model with bidirectional flow interaction between 2D overland surface and 1D sewer networks. In: NOVATECH 2007, Lyon, France.
Chen, A.S., Djordjevic, S., Savic, D., 2016. Urban flash flooding analysis with rain gauge and radar rainfall information. In: ICHE 2016 12th International Conference on Hydroscience & Engineering (November 6).
Cornwall, W., 2021. Europe's deadly floods leave scientists stunned, Science News. https://www.science.org/content/article/europe-s-deadly-floods-leave-scientists-stunned. (Accessed 6 January 2022).
Cox, R.J., Shand, T.D., Blacka, M.J., 2010. Australian rainfall and runoff (AR&R). In: Revision Project 10: Appropriate Safety Criteria for People, Stage 1 Report, pp. 1–33.
Environment Agency, 2013. LIDAR composite DTM 2013. https://environment.data.gov.uk/DefraDataDownload/?Mode=survey.
Evans, B., Chen, A.S., Djordjevic, S., Webber, J., Gómez, A.G., Stevens, J., 2020. Investigating the effects of pluvial flooding and climate change on traffic flows in Barcelona and Bristol. Sustainability 12 (6), 2330. https://doi.org/10.3390/su12062330.
FitzGerald, G., Du, W., Jamal, A., Clark, M., Hou, X.-Y., 2010. Flood fatalities in contemporary Australia (1997–2008). Emerg. Med. Australas. 22, 180–186. https://doi.org/10.1111/j.1742-6723.2010.01284.x.
Hammond, M., Chen, A.S., Djordjević, S., Butler, D., Mark, O., 2015. Urban flood impact assessment: a state-of-the-art. Urban Water J. 12 (1), 14–29. https://doi.org/10.1080/1573062X.2013.857421.
HM Government, 2016. National Flood Resilience Review. HM Government, London, UK.
Jonkman, S.N., Kelman, I., 2005. An analysis of the causes and circumstances of flood disaster deaths. Disasters 29, 75–97. https://doi.org/10.1111/j.0361-3666.2005.00275.x.
Jonkman, S.N., Penning-Rowsell, E., 2008. Human instability in flood flows. J. Am. Water Resour. Assoc. 44, 1208–1218. https://doi.org/10.1111/j.1752-1688.2008.00217.x.
Keller, R.J., Mitsch, B., 1993. Safety aspects of design roadways as floodways. In: Research Report No. 69. Urban Water Research Association of Australia, Melbourne, Australia.
Lam, M.Y., Ahmadian, R., West, C., Pregnolato, M., Evans, B., Chen, A.S., Djordjevic, S., 2022. Evaluating empirical and mechanics-based pedestrian stability models. In: Proceedings of the 39th IAHR World Congress, 19–24 June 2022 Granada, Spain. https://doi.org/10.3850/IAHR-39WC2521711920221560.
Lazzarin, T., Viero, D.P., Molinari, D., Ballio, F., Defina, A., 2022. A new framework for flood damage assessment considering the within-event time evolution of hazard, exposure, and vulnerability. J. Hydrol. 615, 128687 https://doi.org/10.1016/j.jhydrol.2022.128687.
Martínez-Gomariz, E., Gómez, M., Russo, B., 2016. Experimental study of the stability of pedestrians exposed to urban pluvial flooding. Nat. Hazards 82, 1259–1278. https://doi.org/10.1007/s11069-016-2242-z.
Martínez-Gomariz, E., Gómez, M., Russo, B., Djordjević, S., 2017. A new experiments-based methodology to define the stability threshold for any vehicle exposed to flooding. Urban Water J. 14 (9), 930–939. https://doi.org/10.1080/1573062X.2017.1301501.
Melville-Shreeve, P., 2014. Exeter Rain Gauge Record of 16 Oct 2014 Event.
Met Office, 2003. 1 km resolution UK composite rainfall data from the Met Office Nimrod System, NCAS British Atmospheric Data Centre. https://catalogue.ceda.ac.uk/uuid/27dd6ffba67f667a18c62de5c3456350.
Musolino, G., Ahmadian, R., Xia, J., Falconer, R.A., 2020. Mapping the danger to life in flash flood events adopting a mechanics based methodology and planning evacuation routes. J. Flood Risk Manag. 13, e12627 https://doi.org/10.1111/jfr3.12627.
Néelz, S., Pender, G., 2010. Benchmarking of 2D hydraulic modelling packages. https://api.semanticscholar.org/CorpusID:113560957.
Ordnance Survey, 2014. Exeter topography data, using: EDINA Digimap Ordnance Survey Service. http://digimap.edina.ac.uk.
Pregnolato, M., Ford, A., Wilkinson, S.M., Dawson, R.J., 2017. The impact of flooding on road transport: a depth-disruption function. Transp. Res. Part D: Transp. Environ. 55, 67–81. https://doi.org/10.1016/j.trd.2017.06.020.
Pyatkova, K., Chen, A.S., Butler, D., Vojinovic, Z., Djordjevic, S., 2019a. Assessing the knock-on effects of flooding on road transportation. J. Environ. Manag. 244, 48–60. https://doi.org/10.1016/j.jenvman.2019.05.013.
Pyatkova, K., Chen, A.S., Djordjevic, S., Butler, D., Vojinovic, Z., Abebe, Y.A., Hammond, M., 2019b. Flood impacts on road transportation using microscopic traffic modelling techniques. In: Behrisch, M., Weber, M. (Eds.), Simulating Urban Traffic Scenarios. Springer International Publishing, Cham, Switzerland, pp. 115–126. https://doi.org/10.1007/978-3-319-33616-9_8.

Shah, S.M.H., Mustaffa, Z., Martinez-Gomariz, E., Kim, D.K., Yusof, K.W., 2021. Criterion of vehicle instability in floodwaters: past, present and future. Int. J. River Basin Manag. 19 (1), 1–23. https://doi.org/10.1080/15715124.2019.1566240.

Shand, T.D., Cox, R.J., Blacka, M.J., Smith, G.P., 2011. Appropriate safety criteria for vehicles. In: Australian Rainfall and Runoff, P10/S2/020.

Stevens, J., Henderson, R., Webber, J., Evans, B., Chen, A., Djordjević, S., Sánchez-Muñoz, D., Domínguez-García, J.L., 2020. Interlinking Bristol based models to build resilience to climate change. Sustainability 12 (8), 3233. https://doi.org/10.3390/su12083233.

Teo, F.Y., Liew, Y.S., Falconer, R.A., Lin, B.L., 2013. Estimation of Flood Hazard Risk Relating to Vehicles. IAHR World Congress, Chengdu (China).

UN Department of Economic and Social Affairs/Population Division, 2012. World Urbanization Prospects: The 2011 Revision. United Nations, New York.

Vamvakeridou-Lyroudia, L.S., Chen, A.S., Khoury, M., Gibson, M.J., Kostaridis, A., Stewart, D., Wood, M., Djordjevic, S., Savic, D.A., 2020. Assessing and visualising hazard impacts to enhance the resilience of Critical Infrastructures to urban flooding. Sci. Total Environ. 707, 136078 https://doi.org/10.1016/j.scitotenv.2019.136078.

Wang, N., Hou, J., Du, Y., Jing, H., Wang, T., Xia, J., Gong J., Huang M., 2021. A dynamic, convenient and accurate method for assessing the flood risk of people and vehicle. Sci. Total Environ. 797, 149036 https://doi.org/10.1016/j.scitotenv.2021.149036.

Xia, J., Falconer, R.A., Wang, Y., Xiao, X., 2014. New criterion for the stability of a human body in floodwaters. J. Hydraul. Res. IAHR 52, 93–104. https://doi.org/10.1080/00221686.2013.875073.